Proceedings of the 12th World Congress on Electrical Engineering and Computer Systems and Sciences (EECSS'25)
Paris, France – August 17 - 19, 2025
Paper No. ICBES 138
DOI: 10.11159/icbes25.138

Cigarette Smoke-Induced Cell Morphology via Keyence and Zeiss Microscopy

Sarah Li[1, †], Angie Sun[1, †], Yu-Sin (Jennifer) Ou[2], Huiying Huang[1], Wei Sun[3], Veronica Gomez-Godinez[1], Linda Shi[1,*]

[1]Institute of Engineering in Medicine, University of California San Diego, La Jolla, CA, 92093
[2]School of Biological Science, University of California San Diego, La Jolla, CA, 92093
[3]UC San Diego Department of Medicine, La Jolla, CA, 92093
***** Correspondence: zshi@ucsd.edu
†High school students participating in IEM OPALS program

Abstract - Cigarette smoke exposure induces oxidative stress, disrupts gene regulation, and causes morphological alterations in lung epithelial cells. While conventional methods such as qPCR and Western blotting are often used to study these effects, they are costly, labor-intensive, and unsuitable for rapid screening. In this study, we introduce a cost-effective imaging strategy to characterize early cellular responses of human bronchial epithelial cells (HBEpCs) to cigarette smoke extract (CSE). For the first time, the Keyence VHX-7000 digital microscope was employed to systematically analyze CSE-induced morphological changes, with direct comparison to the established Zeiss Axiovert 200M inverted fluorescence microscope. Quantitative analysis revealed consistent trends across both systems, demonstrating that the Keyence platform effectively captures morphological alterations with high throughput and minimal sample preparation. These findings establish the Keyence VHX-7000 as a viable, scalable alternative for preliminary cellular injury assessments, offering a practical tool for accelerating research into smoking-related lung and cardiovascular diseases.

***Keywords*:** Cigarette Smoke Extract (CSE), Human Bronchial Epithelial Cells (HBEpCs), Keyence VHX-7000, Zeiss Axiovert 200M inverted fluorescence microscope, Morphological Analysis, Microscopy Comparison

1. Introduction

Cigarette smoke extract (CSE) induces complex cellular responses, including alterations in gene expression, oxidative stress, and morphological changes, which contribute to the pathological mechanisms underlying smoking-related diseases such as chronic obstructive pulmonary disease (COPD). Chen et al. demonstrated that the COPD susceptibility gene HHIP regulates epithelial repair genes and maintains epithelial-mesenchymal unit integrity in response to cigarette smoke exposure [1]. Chen et al. also showed that N-acetyl-L-cysteine protects lung tissues and alveolar epithelial cells from cigarette smoke-induced oxidative stress by reducing cellular injury [2]. Additionally, Huang et al. found that dietary zinc activates the Nrf2 signaling pathway to inhibit pyroptosis and attenuate lung inflammation in a COPD model [3]. Further, Chen et al. identified mitophagy-related biomarkers in COPD, linking mitochondrial dysfunction to disease progression in cigarette smoke-exposed cells [4].

Recent studies have increasingly utilized human bronchial epithelial cells (HBEpCs) to investigate molecular mechanisms underlying airway diseases. For example, Myszor et al. uncovered critical pathways involved in airway innate immunity [5], Gao et al. studied lung cell apoptosis during pneumonia [6], and Yue et al. explored sepsis-induced lung injury and its impact on lung epithelial apoptosis [7]. These investigations typically relied on molecular biology techniques such as quantitative PCR (qPCR), Western blotting, and immunofluorescence microscopy to assess changes in gene expression, protein abundance, and apoptosis markers under disease-related conditions. While these methods are highly sensitive and regarded as gold standards, they are also expensive, time-consuming, and labor-intensive, requiring costly reagents, specialized equipment, and multi-step workflows that are prone to technical variability.

Our project focuses on investigating how cigarette smoking-induced oxidative stress alters the behavior of microRNAs (miRNAs), shifting its role from cellular protection to promoting disease. Before delving into the complex regulatory effects of miRNAs on DNA repair, inflammation, and cellular senescence, it is critical to first establish an effective concentration of CSE that triggers measurable cellular responses without inducing widespread cell death.

To address this challenge efficiently, we explored, for the first time, the use of the Keyence VHX-7000 high-resolution digital microscope to study the effects of CSE on HBEpCs. Given its cost-effectiveness, ease of use, and ability to rapidly capture high-resolution images, the Keyence system offers a promising alternative to traditional biological imaging platforms. To assess its performance, we directly compared the imaging results and morphological measurements obtained from the Keyence VHX-7000 with those from the widely used Zeiss Axiovert 200M inverted fluorescence microscope. By systematically evaluating the comparability and limitations of the Keyence system, we aim to establish its utility for studying smoking-induced cellular injury, providing a more accessible option for future lung and heart disease research.

While the Keyence VHX-7000 has been successfully utilized in industrial and material science research fields such as coating characterization[8], surface wear analysis[9], and optical surface finishing [10], its application for biological cell imaging has been largely unexplored. In contrast, Zeiss Axiovert microscopes have long been regarded as gold standards for high-resolution imaging in biological and medical research [11-12]. By adapting a commercially available Keyence VHX-7000 system for morphological analysis of HBEpCs, we introduce a cost-effective, high-throughput alternative to conventional biological imaging methods, and directly compare its capabilities and limitations against the established Zeiss Axiovert 200M platform.

2. Materials and Methods

2.1 Cell Preparation

Cryopreserved primary HBEpCs were obtained from Cell Applications, Inc. (Catalog #CA-502-05a) and cultured at 37°C with 5% CO_2 in HBEpC/HTEpC growth medium (Catalog #CA-511K). Cells between passages 3 and 11 were used for all experiments.

For treatments, cells were exposed to 0.3% CSE (Murty Pharmaceuticals, Catalog #MPI-250311) by adding 1.5 µL of CSE to 500 µL of culture medium. Parallel control groups were treated with 0.3% dimethyl sulfoxide (DMSO; Millipore Sigma, Catalog #D2650) at the same dilution. Fixation times were set at 10, 30, 60, and 90 minutes.

2.2 Cell Fixation and Staining

Following treatment, cells were fixed and stained using the following procedure:

1. Allow glutaraldehyde solution to equilibrate to room temperature.
2. Remove culture medium and wash cells three times quickly with phosphate-buffered saline (PBS).
3. Fix cells in 200 µL of 0.25% glutaraldehyde in PBS for 3 minutes at room temperature.
4. Wash cells three times with PBS and maintain them in 1 mL of PBS.
5. Seal dishes with parafilm to prevent evaporation if fixation is paused.
6. Incubate cells with 200 µL of 50 mM glycine solution for 5 minutes to quench residual glutaraldehyde.
7. Add one drop of NucBlue Live ReadyProbes reagent (Thermo Fisher Scientific) for nuclear staining and incubate in the dark for 5 minutes.
8. Wash three times with PBS, disposing of waste in a designated PFA container under a chemical hood.
9. Apply one drop of mounting medium (pre-warmed to room temperature) and carefully place a coverslip without introducing bubbles.
10. Incubate overnight in the dark before transferring to refrigeration for storage.

2.3 High-Resolution Digital Imaging Platforms

In this study, two imaging systems were utilized to characterize the morphological changes in HBEpCs following CSE exposure:

- **Keyence VHX-7000**: It integrates optics, camera, LED illumination, motorized stage, and image processing software into a single system. Features such as high dynamic range (HDR) imaging and real-time depth composition enable fully focused, high-contrast images across irregular surfaces. While traditionally applied to non-biological samples,

this system was evaluated for the first time here to monitor large-scale morphological changes in human epithelial cells.

- **Zeiss Axiovert 200M**: A research-grade inverted fluorescence microscope extensively used in biomedical studies for live-cell imaging, fluorescence microscopy, and high-resolution visualization of cellular structures. It supports a variety of imaging modes (e.g., fluorescence, DIC, phase contrast) and is optimized for biological sample imaging, making it a gold standard for cellular research.

Table 1 lists the comparison of the features of the two systems.

Table 1. Comparison of Keyence VHX-7000 and Zeiss Axiovert 200M for Lung Cell Imaging

Feature/Use Case	Keyence VHX-7000	Zeiss Axiovert 200M
High-Resolution Imaging	✓ Excellent	✓ Excellent
Biological Live-Cell Imaging	✗ Not Suitable	✓ Ideal
Fluorescence Imaging	✗ Not Supported	✓ Strong Capability
Wide Field of View for Morphology	✓ Large-scale capture	✓ Good but more localized
3D Depth Composition (Z-stacking)	✓ Built-in	✓ Possible with accessories
Sample Preparation Requirements	✗ Minimal (dry samples fine)	✓ Required for biological imaging
Cost and Accessibility	$ Cost-effective	$ $ $ Higher cost
Ease of Use	✓ Highly automated	✗ Requires technical expertise

3. Results and discussions

3.1 Morphological Analysis of HBEpCs Using the Keyence VHX-7000 System

This study represents the first systematic application of the Keyence VHX-7000 platform to characterize CSE-induced morphological changes in HBEpCs. The Keyence system, using uniform LED illumination and HDR imaging, allowed acquisition of detailed, high-contrast images for rapid visualization of cell outlines against background substrates. HDR processing further enhanced feature visibility, supporting precise cell size quantification from a single wide-field image that captured hundreds of cells at once. Real-time depth composition was utilized to combine multiple focal planes into fully focused composite images, overcoming the challenges of uneven sample surfaces and enabling clear identification of subtle structural changes and damage induced by CSE treatment.This imaging strategy enabled high-throughput, non-destructive, cost-effective assessment across eight experimental groups: 0.3% CSE or 0.3% DMSO across four time points (10, 30, 60, and 90 minutes). Two imaging modes were utilized: Enhanced Contrast and Enhanced Flaw Detection (Figure 1), allowing clear visualization of cellular boundaries and detection of subtle structural alterations.

Quantitative measurement of the long axis of individual cells revealed no statistically significant differences between CSE and DMSO groups at the 10-, 30-, and 60-minute time points ($p > 0.05$, one-way ANOVA with Tukey's post hoc test). However, at 90 minutes, CSE-treated cells exhibited a significant increase in cell size compared to DMSO controls ($p = 0.037$, unpaired Student's t-test), as shown in Figure 2. This suggests that prolonged exposure to CSE induces measurable morphological changes in epithelial cells, which are detectable using the Keyence platform.

The ability to efficiently capture and analyze hundreds of cells in a single field of view highlights the Keyence system's high-throughput advantage. Its HDR and real-time depth composition features proved effective in resolving morphological features even in slightly uneven culture surfaces.

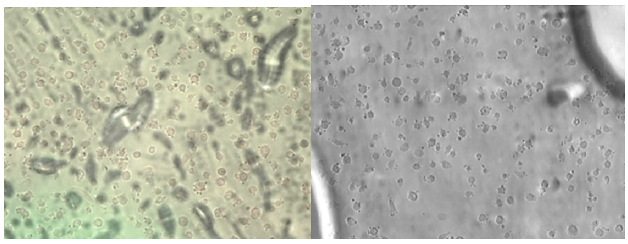

(a) (b)

Figure 1 Keyence Imaging with Enhanced Contrast (a) and Enhanced Flaw (b)

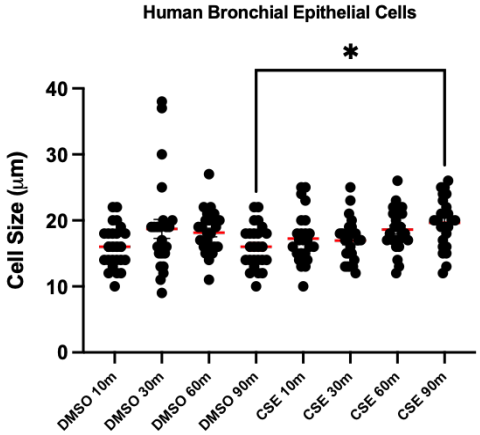

Figure 2 Statistical study of the cell size using the images captured by VHS 7000

3.2 Morphological Analysis of HBEpCs Using Zeiss Axiovert 200M Microscopy

Parallel imaging was performed using the Zeiss Axiovert 200M inverted fluorescence microscope. Cells were visualized using both Phase 3 imaging and Blue Fluorescence Protein (BFP) fluorescence channels to capture morphology and DAPI-stained nuclei, respectively (Figure 3).

Quantitative measurements of the long axis in both phase and fluorescence images were performed using ImageJ. Statistical analysis (Figure 4) revealed comparable findings to those obtained with the Keyence system: minimal differences between CSE and DMSO groups at earlier time points, but significant size changes of cells in the CSE group after 90 minutes.

Notably, measurements from the Zeiss BFP images, which mainly captured nuclear size due to thin cytoplasmic membranes, aligned well with the Keyence measurements. This cross-validation strengthens the reliability of the morphological observations and confirms that both imaging systems, despite differences in optics and sample illumination, captured consistent biological trends.

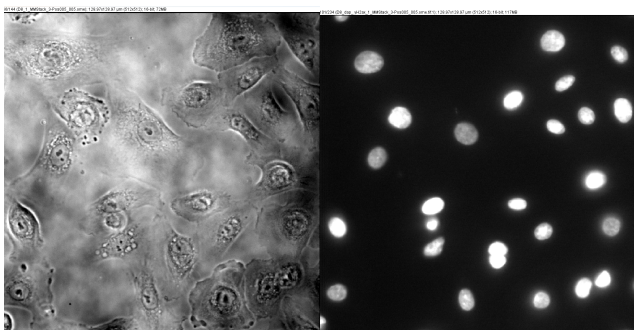

(a) (b)

Figure 3 Images captured under Zeiss Axio 200M Microscope (a) under Phase 3 , (b) DAPI image of (a)

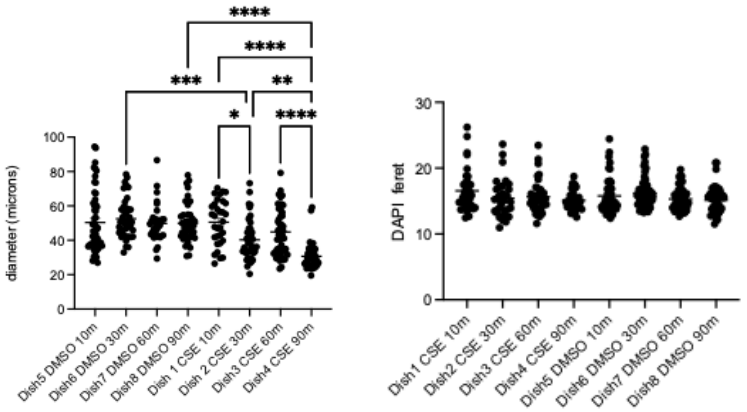

(a) (b)

Figure 4 Statical study of the cell long axis by Zeiss Axio 200M: (a) under Phase 3, (b) under BFP (DAPI image)

4. Conclusion

This study represents the first systematic evaluation of the Keyence VHX-7000 digital microscope for analyzing cigarette smoke extract-induced morphological changes in human bronchial epithelial cells. Our results demonstrate that the Keyence system reliably detects cellular enlargement following prolonged CSE exposure, with measurements closely aligning with those obtained from the gold-standard Zeiss Axiovert 200M system. The Keyence platform offers a high-throughput, cost-effective, and non-destructive imaging solution, significantly reducing the time, labor, and expenses associated with traditional molecular assays. By establishing the Keyence VHX-7000 as a powerful tool for early-phase screening of cellular injury, this work lays the groundwork for broader applications in lung and heart disease research, particularly in studies investigating microRNA regulation under oxidative stress conditions.

Acknowledgements

This material was based upon work supported by a gift from Beckman Laser Institute Inc. to L.S. and V.G.G.. Special thanks to the private donors to our UCSD IEM BTC center: Dr. Shu Chien from UCSD Bioengineering, Dr. Lizhu Chen from CorDx Inc., Dr. Xinhua Zheng, David & Leslie Lee for their generous donations.

References

[1] Chen Q, Wisman M, Nwozor KO, Sin DD, Joubert P, Nickle DC, Brandsma CA, de Vries M, Heijink IH. COPD susceptibility gene HHIP regulates repair genes in airway epithelial cells and repair within the epithelial-mesenchymal trophic unit. Am J Physiol Lung Cell Mol Physiol. 2025 Apr 7. doi: 10.1152/ajplung.00220.2024. Epub ahead of print. PMID: 40192657.

[2] Chen J, Cheng Y, Cui H, Li S, Duan L, Jiao Z. N-acetyl-L-cysteine protects rat lungs and RLE-6TN cells from cigarette smoke-induced oxidative stress. Mol Med Rep. 2025 Apr;31(4):97. doi: 10.3892/mmr.2025.13462. Epub 2025 Feb 21. PMID: 39981906; PMCID: PMC11865697.

[3]Huang Y, Liang T, Liu J, Yu H, Li J, Han L. Dietary Zinc activates the Nrf2 signaling pathway to inhibit pyroptosis and attenuate the lung inflammatory response in COPD. Cytotechnology. 2025 Apr;77(2):62. doi: 10.1007/s10616-025-00725-7. Epub 2025 Feb 18. PMID: 39980839; PMCID: PMC11836256.

[4] Chen J, Zhang X, Sun G. Identification and validation of biomarkers related to mitophagy in chronic obstructive pulmonary disease. Mol Med Rep. 2025 Apr;31(4):93. doi: 10.3892/mmr.2025.13458. Epub 2025 Feb 14. PMID: 39950319; PMCID: PMC11843435.

[5] Myszor IT, Lapka K, Hermannsson K, Rekha RS, Bergman P, Gudmundsson GH. Bile acid metabolites enhance expression of cathelicidin antimicrobial peptide in airway epithelium through activation of the TGR5-ERK1/2 pathway. Sci Rep. 2024 Mar 21;14(1):6750. doi: 10.1038/s41598-024-57251-3. PMID: 38514730; PMCID: PMC10957955.
[6] Gao P, Wang J, Jiang M, Li Z, Xu D, Jing J, Yihepaer, Hu T. LncRNA SNHG16 is Downregulated in Pneumonia and Downregulates miR-210 to Promote LPS-Induced Lung Cell Apoptosis. Mol Biotechnol. 2023 Mar;65(3):446-452. doi: 10.1007/s12033-022-00545-6. Epub 2022 Aug 22. PMID: 35994228.
[7] Yue C, He M, Teng Y, Bian X. Long non-coding RNA metastasis-related lung adenocarcinoma transcript 1 (MALAT1) forms a negative feedback loop with long non-coding RNA colorectal neoplasia differentially expressed (CRNDE) in sepsis to regulate lung cell apoptosis. Bioengineered. 2022 Apr;13(4):8201-8207. doi: 10.1080/21655979.2021.2023727. PMID: 35300579; PMCID: PMC9161944.
[8] Dudek, A., & Kierat, O. (2024). Preliminary Aspects Regarding the Anticorrosive Effect of Multi-Layered Silane–Hydroxyapatite Coatings Deposited on Titanium Grade 2 for Medical Applications. Materials, 17(23), 6001. https://doi.org/10.3390/ma17236001.
[9] Stradomski, G., Fik, J., Lis, Z., Rydz, D., & Szarek, A. (2024). Wear Behaviors of the Surface of Duplex Cast Steel after the Burnishing Process. Materials, 17(8), 1914. https://doi.org/10.3390/ma17081914.
[10] Shrotri, A., Preu, S., & Stübbe, O. (2025). Achieving Transparency and Minimizing Losses of Rough Additively Manufactured Optical Components by a Dip-Coating Surface Finish. Coatings, 15(2), 210. https://doi.org/10.3390/coatings15020210.
[11] Dorn A, Zappe H, Ataman Ç. Conjugate adaptive optics extension for commercial microscopes. Advanced Photonics Nexus. 2024 Sep 1;3(5):056018-.
[12] Wang, P., Liang, J., Shi, L.Z., Wang, Y., Zhang, P., Ouyang, M., Preece, D., Peng, Q., Shao, L., Fan, J., Sun, J., Li, S.S., Berns, M.B., Zhao, H., Wang, Y. Visualizing Spatiotemporal Dynamics of Intercellular Mechanotransmission upon Wounding. ACS Photonics 2018, 5, 3565–3574. https://doi.org/10.1021/acsphotonics.8b00383.